

# Reaction of Silafluorenes with $(\text{Ph}_3\text{P})_2\text{Pt}(\eta^2\text{-C}_2\text{H}_4)$ : Generation and Characterization of Pt–Si Monomers, Dimers, and Trimers

Janet Braddock-Wilking,\* Joyce Y. Corey, Kevin A. Trankler, Kimberly M. Dill,  
Lisa M. French, and Nigam P. Rath

Department of Chemistry and Biochemistry, University of Missouri–St. Louis,  
St. Louis, Missouri 63121

Received March 23, 2004

The reaction of silafluorene (**1**;  $\text{H}_2\text{SiC}_{12}\text{H}_8$ ) with  $(\text{Ph}_3\text{P})_2\text{Pt}(\eta^2\text{-C}_2\text{H}_4)$  (**2**) at room temperature in  $\text{C}_7\text{D}_8$  initially provided the mononuclear complex  $(\text{Ph}_3\text{P})_2\text{Pt}(\text{H})[\text{Si}(\text{H})\text{C}_{12}\text{H}_8]$  (**3**), followed by the appearance of the unsymmetrical dinuclear complex  $(\text{Ph}_3\text{P})_2(\text{H})\text{Pt}(\mu\text{-SiC}_{12}\text{H}_8)(\mu\text{-}\eta^2\text{-HSiC}_{12}\text{H}_8)\text{Pt}(\text{PPh}_3)$  (**4**) and finally the novel trinuclear complex  $[(\text{Ph}_3\text{P})\text{Pt}(\mu\text{-SiC}_{12}\text{H}_8)]_3$  (**5**). The three complexes were characterized by multinuclear NMR spectroscopy and by X-ray crystallography (**5**). The molecular structure of **5** exhibits a nonplanar  $\text{Pt}_3\text{Si}_3$  core. When the reaction was conducted at low temperature until the silafluorene was consumed and the mixture then warmed to room temperature, the dinuclear complex **4** could be isolated. The related substituted silafluorene system 3,7-di-*tert*-butylsilafluorene (**6**;  $\text{H}_2\text{SiC}_{20}\text{H}_{24}$ ) also reacted with **2** to provide both mono- and dinuclear complexes (**7** and **8**) analogous to **3** and **4**. The dinuclear complex **8** was isolated and crystallographically characterized. Each of the two Pt centers in complex **8** exhibits a unique environment. In solution at low temperature **8** is best described as having one platinum center with a terminal hydride,  $[\text{Pt}(\text{H})(\text{PPh}_3)_2]$ , and the second platinum with a nonclassical  $[\text{Si}\cdots\text{H}\cdots\text{Pt}(\text{PPh}_3)]$  unit. However, in the solid state, the two hydrides may both adopt a bridging environment. Heating a sample of the unsymmetrical dimer **8** led to the formation of several products, one of which was the trimer **9**, analogous to **5**.

## Introduction

The study of Si–H bond activation by transition-metal complexes has grown significantly over the last two decades.<sup>1,2</sup> Insertion of a metal center into a Si–H bond is by far the most common and versatile approach for the preparation of compounds containing an M–Si bond.<sup>1</sup> A multitude of ligands both at the metal center and at silicon have been utilized, and all varieties of silanes from  $\text{SiH}_4$  to  $\text{R}_3\text{SiH}$  have been found to react with an appropriate transition-metal precursor for nearly all the metals from groups 3 through 11. The most common type of hydrosilane employed in these reactions is a tertiary hydrosilane ( $\text{R}_3\text{SiH}$ ).<sup>1</sup> However, due to the presence of additional Si–H bonds in primary and secondary silanes further reactions with additional transition-metal centers are possible and such hydrosilanes could be interesting and desirable precursors for Si–H bond activation studies.

Reactions of primary and secondary hydrosilanes with Pt(0) or Pt(II) precursors have provided a variety of structural motifs (see Figure 1).<sup>1</sup> Formal insertion of the metal center into the Si–H bond initially provides a complex with the general formula  $\text{L}_n\text{M}(\text{H})\text{SiR}_3$  (such as **A** in Figure 1).<sup>3</sup> If the groups at silicon and the metal center are not too hindered, then addition of a second hydrosilane is possible and leads (at least formally) to a bis(silyl) complex ( $\text{L}_n\text{M}(\text{SiR}_3)_2$ ; **B** in Figure 1).<sup>3b,d,e,4</sup> Of significance is the observation that, for primary and secondary hydrosilanes, the additional sites of reactivity from residual hydrides at the bound silicon center can give rise to dinuclear or higher order metal clusters. Dinuclear complexes containing bridging silylene units (**C**)<sup>3e,4a,5,6,7b</sup> as well as dinuclear species having nonclassical  $\text{Pt}\cdots\text{H}\cdots\text{Si}$  interactions<sup>8</sup> (**D**)<sup>3b,5g,7</sup> and **E** (including this work and a related dipalladium system<sup>9</sup>) have now been prepared. These will be referred to as symmetrical (**D**) and unsymmetrical (**E**) dimers, respectively, through-

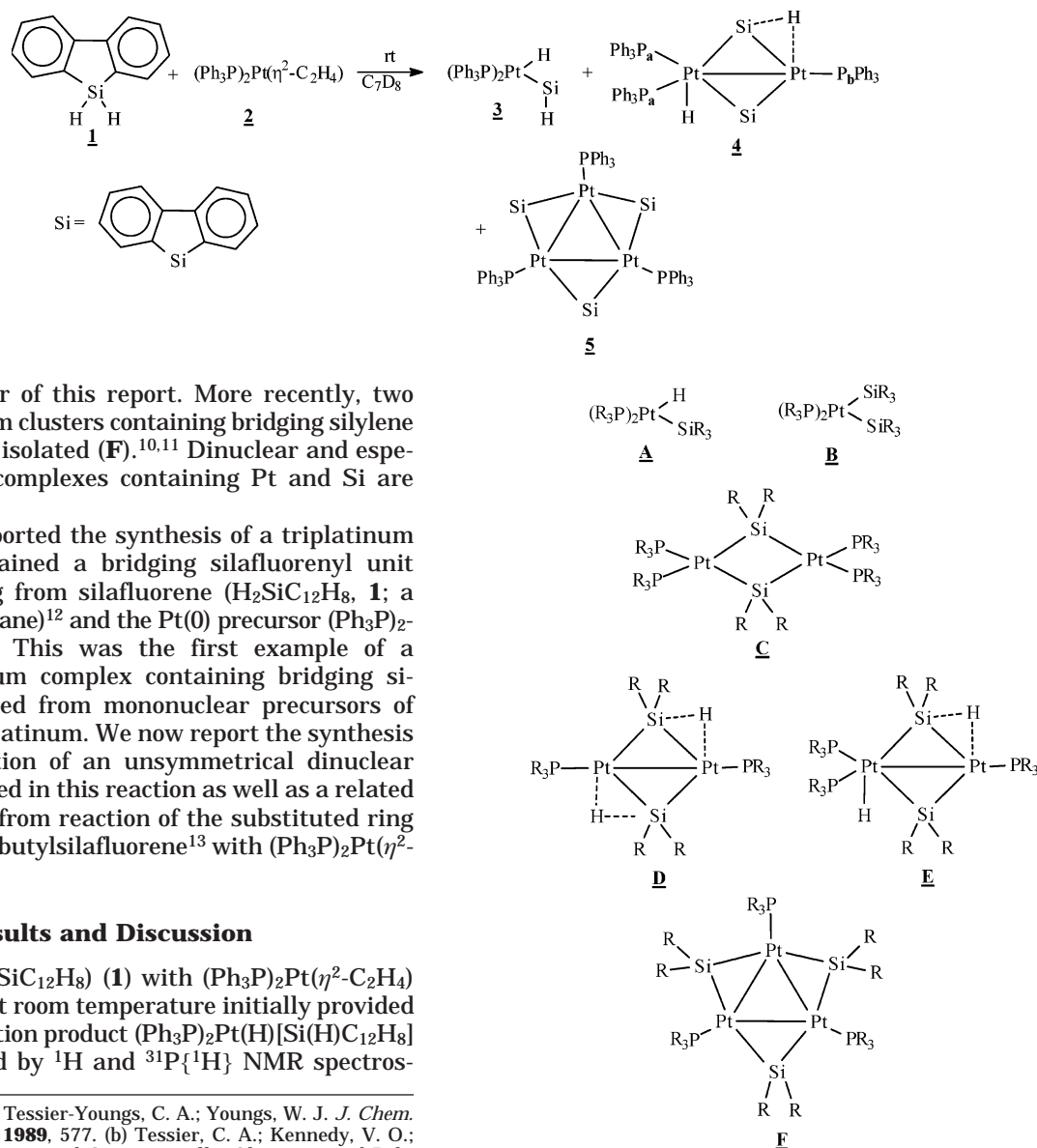
(1) Corey, J. Y.; Braddock-Wilking, J. *Chem. Rev.* **1999**, *99*, 175.

(2) For selected general reviews on transition-metal silyl complexes see: (a) Tilley, T. D. Transition-Metal Silyl Derivatives. In *The Chemistry of Organic Silicon Compounds*; Patai, S., Rappoport, Z., Eds.; Wiley: New York, 1989; p 1416. (b) Tilley, T. D. Appendix to Transition-Metal Silyl Derivatives. In *The Silicon-Heteroatom Bond*; Patai, S., Rappoport, Z., Eds.; Wiley: New York, 1991; p 309. (c) Schubert, U. *Transition Met. Chem.* **1991**, *16*, 136. (d) Schubert, U. Activation of Si–X Bonds by Electron-Deficient Transition Metals. In *Progress in Organosilicon Chemistry*; Marciniec, B., Chojnowski, J., Eds.; Gordon and Breach: Lausanne, Switzerland, 1995; p 287. (e) Eisen, M. S. Transition-Metal Silyl Complexes. In *The Chemistry of Organic Silicon Compounds*; Wiley: New York, 1998; Vol. 2, Part 3, p 2037. (f) Aylett, B. J. *Adv. Inorg. Chem. Radiochem.* **1982**, *25*, 1.

(3) For selected recent examples involving primary and secondary hydrosilanes see: (a) Simons, R. S.; Sanow, L. M.; Galat, K. J.; Tessier, C. A.; Youngs, W. J. *Organometallics* **2000**, *19*, 3994. (b) Braddock-Wilking, J.; Levchinsky, Y.; Rath, N. P. *Organometallics* **2000**, *19*, 5500. (c) Feldman, J. D.; Mitchell, G. P.; Nolte, J.-O.; Tilley, T. D. *J. Am. Chem. Soc.* **1998**, *120*, 11184. (d) Kim, Y.-J.; Park, J.-I.; Lee, S.-C.; Osakada, K.; Tanabe, M.; Choi, J.-C.; Koizumi, T.; Yamamoto, T. *Organometallics* **1999**, *18*, 1349. (e) Heyn, R. H.; Tilley, T. D. *J. Am. Chem. Soc.* **1992**, *114*, 1917.

(4) (a) Shimada, S.; Tanaka, M.; Honda, K. *J. Am. Chem. Soc.* **1995**, *117*, 8289. (b) Michalczyk, M. J.; Recatto, C. A.; Calabrese, J. C.; Fink, M. J. *J. Am. Chem. Soc.* **1992**, *114*, 7955. (c) Schubert, U.; Kalt, D.; Gilges, H. *Monatsh. Chem.* **1999**, *130*, 207.

## Scheme 1



out the remainder of this report. More recently, two trinuclear platinum clusters containing bridging silylene groups have been isolated (**F**).<sup>10,11</sup> Dinuclear and especially trinuclear complexes containing Pt and Si are quite rare.<sup>6</sup>

We recently reported the synthesis of a triplatinum cluster that contained a bridging silafluorenyl unit ( $\text{SiC}_{12}\text{H}_8$ ) starting from silafluorene ( $\text{H}_2\text{SiC}_{12}\text{H}_8$ , **1**; a secondary hydrosilane)<sup>12</sup> and the Pt(0) precursor  $(\text{Ph}_3\text{P})_2\text{Pt}(\eta^2\text{-C}_2\text{H}_4)$  (**2**).<sup>11</sup> This was the first example of a trinuclear platinum complex containing bridging silylene units formed from mononuclear precursors of both silicon and platinum. We now report the synthesis and characterization of an unsymmetrical dinuclear complex also formed in this reaction as well as a related dinuclear system from reaction of the substituted ring system 3,7-di-*tert*-butylsilafluorene<sup>13</sup> with  $(\text{Ph}_3\text{P})_2\text{Pt}(\eta^2\text{-C}_2\text{H}_4)$ .

## Results and Discussion

Reaction of  $(\text{H}_2\text{SiC}_{12}\text{H}_8)$  (**1**) with  $(\text{Ph}_3\text{P})_2\text{Pt}(\eta^2\text{-C}_2\text{H}_4)$  (**2**) (ca. 1:1 ratio) at room temperature initially provided the oxidative-addition product  $(\text{Ph}_3\text{P})_2\text{Pt}(\text{H})[\text{Si}(\text{H})\text{C}_{12}\text{H}_8]$  (**3**), as determined by  $^1\text{H}$  and  $^{31}\text{P}\{^1\text{H}\}$  NMR spectro-

(5) (a) Zarate, E. A.; Tessier-Youngs, C. A.; Youngs, W. J. *J. Chem. Soc., Chem. Commun.* **1989**, 577. (b) Tessier, C. A.; Kennedy, V. O.; Zarate, E. A. In *Inorganic and Organometallic Oligomers and Polymers*; Harrod, J. F., Laine, R. M., Eds.; Kluwer Academic: Dordrecht, The Netherlands, 1991; p 13. (c) Anderson, A. B.; Shiller, P.; Zarate, E. A.; Tessier-Youngs, C. A.; Youngs, W. J. *Organometallics* **1989**, *8*, 2320. (d) Zarate, E. A.; Tessier-Youngs, C. A.; Youngs, W. J. *J. Am. Chem. Soc.* **1988**, *110*, 4068. (e) Levchinsky, Y.; Rath, N. P.; Braddock-Wilking, J. *Organometallics* **1999**, *18*, 2583. (f) Braddock-Wilking, J.; Levchinsky, Y.; Rath, N. P. *Organometallics* **2001**, *20*, 474. (g) Sanow, L. M.; Chai, M.; McConville, D. B.; Galat, K. J.; Simons, R. S.; Rinaldi, P. L.; Youngs, W. J.; Tessier, C. A. *Organometallics* **2000**, *19*, 192. (h) Braddock-Wilking, J.; Levchinsky, Y.; Rath, N. P. *Inorg. Chim. Acta* **2002**, *330*, 82. (i) Tanabe, M.; Osakada, K. *Inorg. Chim. Acta* **2003**, *350*, 201.

(6) Ogino, H.; Tobita, H. *Adv. Organomet. Chem.* **1998**, *42*, 223.

(7) (a) Auburn, M.; Ciriano, M.; Howard, J. A. K.; Murray, M.; Pugh, N. J.; Spencer, J. L.; Stone, F. G. A.; Woodward, P. *J. Chem. Soc., Dalton Trans.* **1980**, 659. (b) Tanabe, M.; Yamada, T.; Osakada, K. *Organometallics* **2003**, *22*, 2190.

(8) Schubert, U. *Adv. Organomet. Chem.* **1990**, *30*, 151.

(9) (a) Kim, Y.-J.; Lee, S.-C.; Park, J.-I.; Osakada, K.; Choi, J.-C.; Yamamoto, T. *Organometallics* **1998**, *17*, 4929. (b) Kim, Y.-J.; Lee, S.-C.; Park, J.-I.; Osakada, K.; Choi, J.-C.; Yamamoto, T. *Dalton* **2000**, 417.

(10) Osakada, K.; Tanabe, M.; Tanase, T. *Angew. Chem., Int. Ed.* **2000**, *39*, 4053.

(11) Braddock-Wilking, J.; Corey, J. Y.; Dill, K.; Rath, N. P. *Organometallics* **2002**, *21*, 5467.

(12) (a) Chang, L. S.; Corey, J. Y. *J. Organomet. Chem.* **1986**, *307*, 7. (b) For a recent report on the synthesis of dichlorosilafluorene see:

Liu, Y.; Stringfellow, T. C.; Ballweg, T.; Guzei, I. A.; West, R. *J. Am. Chem. Soc.* **2002**, *124*, 49.

(13) Chang, L. S.; Corey, J. Y. *Organometallics* **1989**, *8*, 1885.

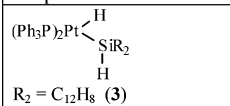
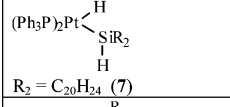
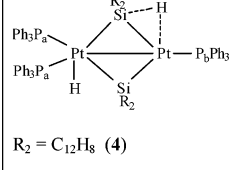
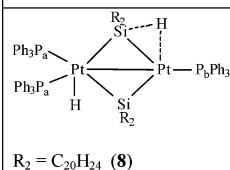
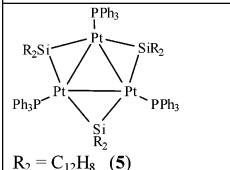
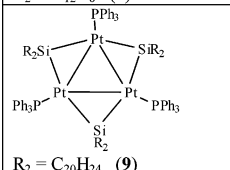
**Figure 1.** Various structural motifs formed from Si–H bond activation at Pt(0).

copy. The composition of the reaction mixture changed over time, and the products that evolved are summarized in Scheme 1. Characterization of each of the complexes is described in the following paragraphs. Table 1 lists the various products formed in this study along with selected NMR spectroscopic data for each complex.

Complex **3** was characterized in solution only ( $\text{C}_7\text{D}_8$ ). Two different  $^{31}\text{P}$  resonances were observed as doublets at 33.9 and 34.2 ppm, both with platinum satellites. In addition, a sharp doublet of doublets with platinum satellites was observed at  $-1.72$  ppm in the  $^1\text{H}$  spectrum. The remaining silicon-bound hydride in **3** was tentatively assigned to a resonance at 5.1 ppm that overlapped the resonance due to free  $\text{C}_2\text{H}_4$ .<sup>14</sup> After approximately 30 min the NMR signals for **3** disappeared and a new broad resonance (ca. 20 ppm) intensi-

(14) Attempts to confirm the position of this resonance by 2D NMR spectroscopy failed, due to the limited lifetime of **3**.

**Table 1. Comparison of Selected NMR Spectroscopic Data for Complexes 3–5 and 7–9**

complex	$^1\text{H}$ NMR data <sup>a</sup>	$^{31}\text{P}\{^1\text{H}\}$ NMR data <sup>a</sup>	$^{29}\text{Si}\{^1\text{H}\}$ NMR data <sup>a</sup>
 $\text{R}_2 = \text{C}_{12}\text{H}_8$ ( <b>3</b> )	$\overline{\text{rt}}$ -1.72 (dd, $^1J_{\text{PtH}} = 956$ , $^2J_{\text{PtH}} = 156$ ( <i>trans</i> ), 21 ( <i>cis</i> )) 5.1 (m overlapping with $\text{C}_2\text{H}_4$ , SiH) <sup>b</sup> -50 °C -1.61 (br d, $^1J_{\text{PtH}} = 945$ , $^2J_{\text{PtH}} = 140$ ) 6.56 (br s, $^2J_{\text{PtH}} = 56$ , SiH) <sup>c</sup>	$\overline{\text{rt}}$ 34.2 (d, $^1J_{\text{PtP}} = 1883$ , $^2J_{\text{PP}} = 8$ ) 33.9 (d, $^1J_{\text{PtP}} = 2537$ )	n/a
 $\text{R}_2 = \text{C}_{20}\text{H}_{24}$ ( <b>7</b> )	-50 °C -1.26 (dd, $^1J_{\text{PtH}} = ^2J_{\text{PtH}} = 152$ ( <i>trans</i> ), 19 ( <i>cis</i> )) 7.07 <sup>b,c</sup>	-50 °C 35.1 (d, $^1J_{\text{PtP}} = 1876$ , $^2J_{\text{PP}} = 10$ ) 33.6 (d, $^1J_{\text{PtP}} = 2558$ )	-50 °C -18.5 (dd, $^1J_{\text{PtSi}} = 1105$ , $^2J_{\text{PtSi}} = 154$ ( <i>trans</i> ), 11 ( <i>cis</i> ))
 $\text{R}_2 = \text{C}_{12}\text{H}_8$ ( <b>4</b> )	$\overline{\text{rt}}$ <sup>d</sup> -50 °C 2.0 (d, $^2J_{\text{PtH}} = 12$ ) <sup>b</sup> -4.9 (t, $^1J_{\text{PtH}} = 577$ , $^2J_{\text{PtH}} \sim 80$ , $^2J_{\text{PH}} = 10$ )	$\overline{\text{rt}}$ 14 (br s) -50 °C 31.1 (t, $^1J_{\text{PtP}} = 4260$ , $^2J_{\text{PtP}} = 265$ , $^3J_{\text{PP}} = 25$ ) 17.3 (d, $^1J_{\text{PtP}} = 3438$ , $^2J_{\text{PtP}} = 135$ )	$\overline{\text{rt}}$ 156 (s, $J_{\text{PtSi}} = 1374$ , 376) -50 °C <sup>b</sup> 160 (d, $^2J_{\text{PtSi}} = 96$ ) 151 (prob t)
 $\text{R}_2 = \text{C}_{20}\text{H}_{24}$ ( <b>8</b> )	$\overline{\text{rt}}$ <sup>d</sup> -50 °C 1.93 (d, $^2J_{\text{PtH}} = 12$ ) -5.2 (t, $^1J_{\text{PtH}} = 572$ , $^2J_{\text{PtH}} \sim 90$ , $^2J_{\text{PH}} = 9$ )	$\overline{\text{rt}}$ 24 (br) -50 °C 30.3 (t, $^1J_{\text{PtP}} = 4171$ , $^2J_{\text{PtP}} = 278$ , $^3J_{\text{PP}} = 26$ ) 21.5 (d, $^1J_{\text{PtP}} = 3504$ ) <sup>c</sup>	$\overline{\text{rt}}$ 158 (s, $J_{\text{PtSi}} = 1332$ , 358) -50 °C <sup>b</sup> 164 (d, $^2J_{\text{PtSi}} = 94$ ) 154 (m)
 $\text{R}_2 = \text{C}_{12}\text{H}_8$ ( <b>5</b> )	$\overline{\text{rt}}$ <sup>d</sup>	$\overline{\text{rt}}$ 70.5 (s, $^1J_{\text{PtP}} = 3338$ , $^2J_{\text{PtP}} = 421$ , $^3J_{\text{PP}} = 80$ )	$\overline{\text{rt}}$ 269 (s, $^1J_{\text{PtSi}} = 934$ )
 $\text{R}_2 = \text{C}_{20}\text{H}_{24}$ ( <b>9</b> )	$\overline{\text{rt}}$ <sup>d</sup>	71.6 (s, $^1J_{\text{PtP}} = 3320$ , $^2J_{\text{PtP}} = 445$ , $^3J_{\text{PP}} = 81$ )	n/a

<sup>a</sup>  $\text{C}_7\text{D}_8$  solution. Chemical shifts are given in ppm and coupling constants in Hz. Si–H coupling not resolved. <sup>b</sup> Pt satellites not resolved. <sup>c</sup> Resonance located by 2D  $^1\text{H}$ – $^{29}\text{Si}$  HMQC experiment. <sup>d</sup> No hydrides observed. <sup>e</sup>  $^2J_{\text{PtP}}$  not resolved.

fied in the  $^{31}\text{P}\{^1\text{H}\}$  spectrum and was accompanied by a broad resonance in the  $^1\text{H}$  spectrum at  $-1$  ppm with platinum satellites. A low-temperature  $^{31}\text{P}\{^1\text{H}\}$  NMR experiment provided resolved signals which were assigned to the unusual dinuclear complex **4**. An isolated sample of **4**, when redissolved, showed peaks identical with those observed in the  $^{31}\text{P}\{^1\text{H}\}$  spectra (223 K) obtained from the original reaction mixture containing **4** (see Experimental Section and Table 1). However, no hydride resonances associated with **4** were observed in the  $^1\text{H}$  spectrum of the isolated sample at room temperature.

Two distinct resonances were observed at 17.3 and 31.1 ppm for **4** in the  $^{31}\text{P}\{^1\text{H}\}$  NMR spectrum (223 K in  $\text{C}_7\text{D}_8$ ) as a doublet and triplet, respectively, in a 2:1 ratio, and each exhibited two sets of Pt satellites (Figure 2a). The doublet resonance is assigned to the two equivalent phosphines ( $\text{P}_a$ ) which couple to the unique phosphine ( $\text{P}_b$ ). Coupling between these two phosphine sites was confirmed by a 2D  $^{31}\text{P}$ – $^{31}\text{P}\{^1\text{H}\}$  COSY experiment.

The  $^1\text{H}$  NMR spectrum (223 K in  $\text{C}_7\text{D}_8$ ) for **4** exhibited two distinct hydride signals centered at  $-4.9$  (t, with

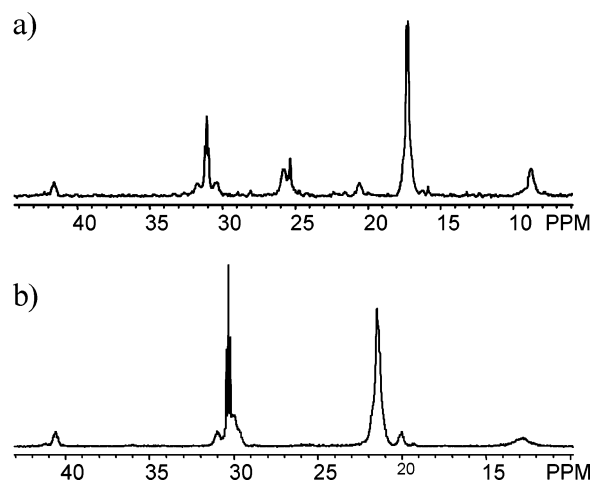


**Figure 2.**  $^{31}\text{P}\{^1\text{H}\}$  NMR data (202 MHz, 223 K,  $\text{C}_7\text{D}_8$ ) for (a) **4** and (b) **8**.

two sets of Pt satellites) and 2.0 ppm (d, Pt satellites not resolved) (Figure 3a shows the upfield hydride region for **4**). The triplet pattern at  $-4.9$  ppm indicates that the hydride couples equivalently to two phosphines,

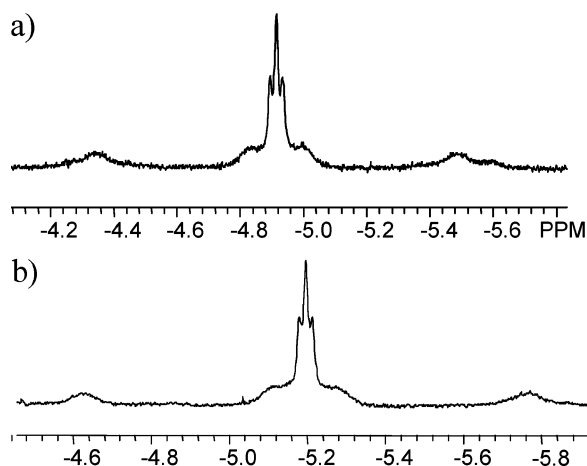


**Figure 3.** Selected  $^1\text{H}$  NMR data (500 MHz, 223 K,  $\text{C}_7\text{D}_8$ ) for (a) **4** and (b) **8**, showing terminal hydride regions.

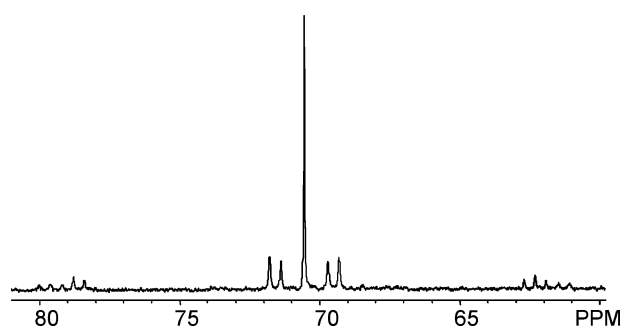


**Figure 4.**  $^{31}\text{P}\{^1\text{H}\}$  NMR data (202 MHz, 223 K,  $\text{C}_7\text{D}_8$ ) for **5**.

and the higher field resonance suggests that this hydride is terminal in nature. The downfield resonance for the other hydride appears in the typical range for bridging nonclassical  $\text{Pt}\cdots\text{H}\cdots\text{Si}$  interactions.<sup>3b,5g,7</sup> Furthermore, the  $^{29}\text{Si}\{^1\text{H}\}$  NMR spectrum (223 K) showed two peaks at 151 (probable t) and 160 (d) ppm, indicating two different silicon centers. The room-temperature  $^{29}\text{Si}\{^1\text{H}\}$  spectrum showed an averaged signal with Pt satellites for the two silicon centers at 156 ppm. Attempts to obtain **4** in crystalline form suitable for X-ray analysis have been unsuccessful.

The reaction mixture was continuously monitored by NMR spectroscopy over a period of several hours. Over the course of 2–3 h an additional new resonance intensified in the  $^{31}\text{P}\{^1\text{H}\}$  NMR spectrum (room temperature) at 70.5 ppm as a singlet with a complex Pt satellite pattern (Figure 4).<sup>15</sup> This resonance was assigned to the trinuclear Pt complex **5**, which was isolated as a deep red solid. The  $^1\text{H}$  NMR spectrum for **3** exhibited only aromatic resonances in the range from 7.4 to 6.07 ppm. No signals were observed that could be attributed to a terminal or bridging hydride in **5**. To verify this, the reaction of  $d_2$ -silafluorene with  $(\text{Ph}_3\text{P})_2\text{Pt}(\eta^2\text{-C}_2\text{H}_4)$  was monitored by  $^2\text{H}$  NMR spectroscopy and no resonances for either bridging or terminal metal deuterides that could be attributed to **5** were detected.<sup>16</sup> In addition, a  $^{29}\text{Si}\{^1\text{H}\}$  resonance was observed at

(15) The satellite pattern observed in the  $^{31}\text{P}\{^1\text{H}\}$  NMR spectrum for **5** is in good agreement with a calculated spectrum for the related triplatinum complex  $\text{Pt}_3(\mu\text{-CO})_3(\text{PCy}_3)_3$ . See: Moor, A.; Pregosin, P. S.; Venanzi, L. M. *Inorg. Chim. Acta* **1981**, *48*, 153.

(16) Braddock-Wilking, J.; Corey, J. Y.; Dill, K. M. Unpublished results.

significantly low field (269 ppm) and is close to the value reported for the related complex  $[(\text{Me}_3\text{P})\text{Pt}(\mu\text{-SiPh}_2)]_3$  (279 ppm).<sup>10</sup> Thus, all spectroscopic data for **5** are in agreement with a trimer species in solution.

The reactivity of the aryl-substituted silafluorene system 3,7-di-*tert*-butylsilafluorene (**6**)<sup>13</sup> with  $(\text{Ph}_3\text{P})_2\text{Pt}(\eta^2\text{-C}_2\text{H}_4)$  (**2**) was also examined. Our goals for studying this hydrosilane were 3-fold. Increased solubility in hydrocarbon solvents should be observed, due to the presence of *tert*-butyl groups on the aromatic rings meta to the silicon. Second, the *t*-Bu groups could potentially provide an additional NMR probe for  $^1\text{H}$  NMR analyses. Another advantage of using the *tert*-butyl groups may be the additional steric bulk slightly away from the silicon center that would still allow reaction with the Pt complex. The presence of the *t*-Bu substituents could kinetically stabilize any reactive intermediate that may be generated and that may otherwise not be observed in the parent silafluorene system.

The room-temperature reaction between  $(\text{Ph}_3\text{P})_2\text{Pt}(\eta^2\text{-C}_2\text{H}_4)$  (**2**) and 3,7-di-*tert*-butylsilafluorene (**6**) was monitored by  $^1\text{H}$  and  $^{31}\text{P}\{^1\text{H}\}$  NMR spectroscopy. Addition of **6** to **2** (both in  $\text{C}_7\text{D}_8$  solution) resulted in vigorous bubbling, followed by darkening of the solution to an amber red. The NMR spectroscopic analysis of the reaction mixture indicated the formation of the dinuclear species **8** as the major product (Scheme 2), as confirmed by low-temperature  $^1\text{H}$  and  $^{31}\text{P}\{^1\text{H}\}$  NMR spectroscopy. No resonances for a mononuclear species analogous to **3** were observed at room temperature. However, when the addition was performed at lower temperature (223 K), signals for the monomer **7** could be observed in both the  $^1\text{H}$  and  $^{31}\text{P}\{^1\text{H}\}$  NMR spectra (see Table 1).<sup>17</sup>

Approximately 10 min after the mixing of the components, the  $^{31}\text{P}\{^1\text{H}\}$  spectrum showed a broad resonance centered at 24 ppm (range 10–30 ppm). No resolved hydride resonances for **8** were observed at room temperature. However, upon cooling to 223 K, the  $^1\text{H}$  NMR spectrum displayed two distinct hydride resonances. An upfield signal at –5.2 ppm was observed as a triplet with two sets of Pt satellites and was assigned to a hydride bound to the  $\text{Pt}(\text{PPh}_3)_2$  ( $\text{P}_a$ ) center. Another hydride was observed at 1.93 ppm as a doublet, which was assigned to the bridging hydride associated with the monophosphine platinum center ( $\text{PtP}_b$ ), but Pt satellites could not be resolved due to overlapping resonances. Figure 3b shows the upfield hydride region in the  $^1\text{H}$  NMR spectrum for **8**. On the basis of the chemical shifts and the observed coupling constants, we assign the upfield hydride resonance to a terminal hydride unit and the downfield hydride as bridging the Pt and silicon centers (a  $\text{Pt}\cdots\text{H}\cdots\text{Si}$  nonclassical interaction).

The  $^{31}\text{P}\{^1\text{H}\}$  NMR spectrum for **8** at 223 K showed two unique resonances: one at 21.5 ppm as a broadened singlet with satellites and a second at 30.3 ppm as a triplet with Pt satellites. These resonances were observed in a 2:1 ratio and were assigned to the equivalent phosphines ( $\text{P}_a$ ,  $(\text{Ph}_3\text{P}_a)_2\text{Pt}$ ) and unique phosphine ( $\text{P}_b$ ,  $(\text{Ph}_3\text{P}_b)\text{Pt}$ ) centers, respectively. Figure 2b shows the low-temperature  $^{31}\text{P}\{^1\text{H}\}$  NMR spectrum of **8**.

(17) Variable-temperature reaction conditions are currently being examined with both the unsubstituted and substituted silafluorene systems **1** and **6** to monitor the sequence of steps.

## Scheme 2

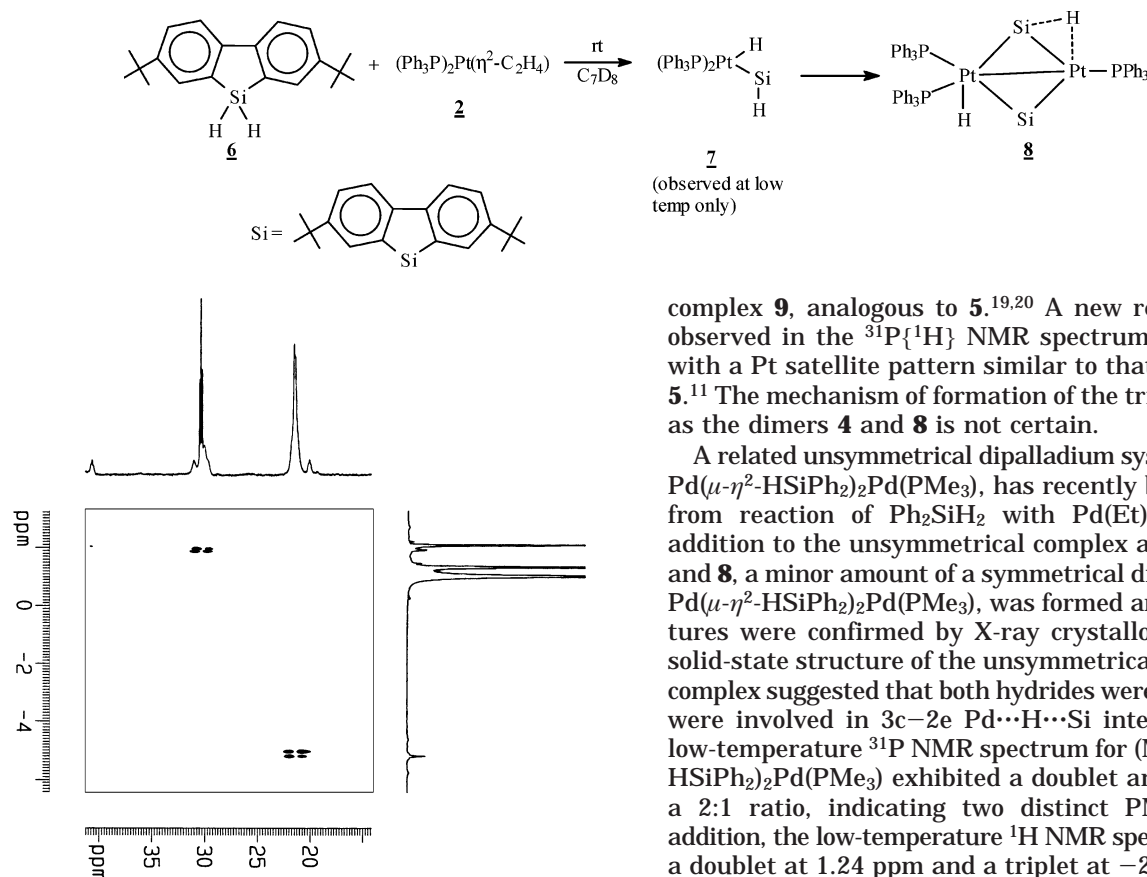


**Figure 5.**  $^1\text{H}$ – $^{31}\text{P}$  COSY NMR data (500 MHz, 223 K,  $\text{C}_7\text{D}_8$ ) for **8**.

A two-dimensional  $^{31}\text{P}$ – $^{31}\text{P}\{^1\text{H}\}$  COSY NMR experiment confirmed coupling between the two phosphorus sites. In addition, a  $^1\text{H}$ – $^{31}\text{P}$  COSY experiment showed correlation only between the triplet phosphorus signal at 30 ppm (for the unique phosphine) and the bridging hydride at 1.93 ppm in the  $^1\text{H}$  spectrum (Figure 5). Likewise, the doublet resonance in the  $^{31}\text{P}$  spectrum assigned to the two equivalent  $\text{PPh}_3$  groups ( $\text{P}_a$ ) showed a correlation only to the terminal hydride found at –5.2 ppm in the  $^1\text{H}$  spectrum. The IR spectrum of **8** showed no absorbances between 2000 and 2300  $\text{cm}^{-1}$ , suggesting that in the solid state no terminal  $\text{Pt}$ – $\text{H}$  or  $\text{Si}$ – $\text{H}$  units exist.<sup>18</sup>

The  $^{29}\text{Si}\{^1\text{H}\}$  NMR spectrum (223 K) also supported the unsymmetrical nature of **8**. Two resonances were observed at 164 (d) and 154 (m) ppm, indicating two different silicon centers in **8**. The  $\text{Pt}$ – $\text{Si}$  couplings could not be resolved in the low-temperature spectrum.

An interesting observation from the reaction of **6** and **2** conducted at room temperature was the fact that no trimer analogous to **5** formed. The *m*-*tert*-butyl groups on the aromatic ring system in **8** may provide sufficient steric bulk to prevent formation of a trinuclear system (at room temperature). However, heating a toluene- $d_8$  sample of **8** at 100 °C overnight provided NMR spectroscopic evidence for the formation of the trinuclear

complex **9**, analogous to **5**.<sup>19,20</sup> A new resonance was observed in the  $^{31}\text{P}\{^1\text{H}\}$  NMR spectrum at 71.6 ppm with a Pt satellite pattern similar to that exhibited by **5**.<sup>11</sup> The mechanism of formation of the trimer **5** as well as the dimers **4** and **8** is not certain.

A related unsymmetrical dipalladium system,  $(\text{Me}_3\text{P})_2\text{-Pd}(\mu\text{-}\eta^2\text{-HSiPh}_2)_2\text{Pd}(\text{PMe}_3)$ , has recently been reported from reaction of  $\text{Ph}_2\text{SiH}_2$  with  $\text{Pd}(\text{Et})_2(\text{PMe}_3)_2$ .<sup>9</sup> In addition to the unsymmetrical complex analogous to **4** and **8**, a minor amount of a symmetrical dimer,  $[(\text{Me}_3\text{P})\text{-Pd}(\mu\text{-}\eta^2\text{-HSiPh}_2)_2\text{Pd}(\text{PMe}_3)]_2$ , was formed and both structures were confirmed by X-ray crystallography.<sup>9</sup> The solid-state structure of the unsymmetrical dipalladium complex suggested that both hydrides were bridging and were involved in  $3c\text{-}2e$   $\text{Pd}\cdots\text{H}\cdots\text{Si}$  interactions. The low-temperature  $^{31}\text{P}$  NMR spectrum for  $(\text{Me}_3\text{P})\text{Pd}(\mu\text{-}\eta^2\text{-HSiPh}_2)_2\text{Pd}(\text{PMe}_3)$  exhibited a doublet and a triplet in a 2:1 ratio, indicating two distinct  $\text{PMe}_3$  sites. In addition, the low-temperature  $^1\text{H}$  NMR spectrum showed a doublet at 1.24 ppm and a triplet at –2.34 ppm with  $^1J_{\text{SiH}}$  couplings of 84 and 86 Hz, respectively. The high-field signal was assigned to the  $(\text{Me}_3\text{P})\text{Pd}\cdots\text{H}\cdots\text{SiPh}_2$  hydride on the basis of the coupling pattern, which suggested that  $^2J_{\text{PH}}$  coupling through Pd was probably much smaller due to the elongated  $\text{Pd}$ – $\text{H}$  distance.<sup>9a</sup> The unsymmetrical palladium dimer was found to have temperature-dependent NMR spectra, and a fluxional exchange of the coordinated  $\text{PMe}_3$  ligands was proposed.<sup>9</sup> A similar process may be responsible for the fluxional behavior found in **4** and **8**.

**X-ray Crystallographic Analyses of 5 and 8.** X-ray-quality crystals of **5** were obtained by slow evaporation from a toluene solution. The deep red crystals of **5**, however, provided reduced quality structural data and only allowed for evaluation of the basic features of the molecule.<sup>11</sup> Figure 6 shows the core structure for the complex **5**. Figure 7 shows selected bond distances for **5** as well as the related trimer  $[(\text{Me}_3\text{P})\text{Pt}(\mu\text{-SiPh}_2)]_3$ .<sup>10</sup> Also given in Figure 7 are selected bond distances for the unsymmetrical dimer (**8**; see discussion below) and the related dipalladium complex  $(\text{Me}_3\text{P})_2\text{Pd}(\mu\text{-}\eta^2\text{-HSiPh}_2)_2\text{Pd}(\text{PMe}_3)$ .<sup>9a</sup>

(19) Trankler, K.; Braddock-Wilking, J.; Corey, J. Y. Unpublished results. A  $^{31}\text{P}\{^1\text{H}\}$  NMR spectrum showed a major component with a signal at 71.6 ppm, which has been assigned to the trinuclear complex **9**. The coupling constant values for **9** are similar to those of the trimer **5**. In addition, several other unassigned resonances were observed to those for **9**. Experiments are in progress to identify and characterize **9** and other products formed in the reaction. One product that has been assigned is the previously characterized phosphido-bridged dimer  $[(\text{Ph}_3\text{P})\text{Pt}(\mu\text{-PPh}_2)]_2$ .<sup>20</sup>

(20) (a) Taylor, N. J.; Chieh, P. C.; Carty, A. J. *J. Chem. Soc., Chem. Commun.* **1975**, 448. (b) Bender, R.; Bouaoud, S.-E.; Braunstein, P.; Dusausoy, Y.; Merabet, N.; Raya, J.; Rouag, D. *J. Chem. Soc., Dalton Trans.* **1999**, 735.

(18) (a) Nakamoto, K. *Infrared and Raman Spectra of Inorganic and Coordination Compounds*; 4th ed.; Wiley: New York, 1986; pp 323, 384, 399. (b) Collman, J. P.; Hegedus, L. S.; Norton, J. R.; Finke, R. G. *Principles and Applications of Organotransition Metal Chemistry*; University Science Books: Mill Valley, CA, 1987; p 83.

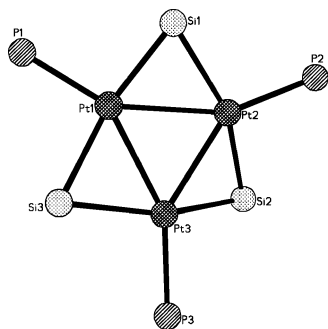


**Figure 6.** Molecular structure of **5** showing the core atoms.

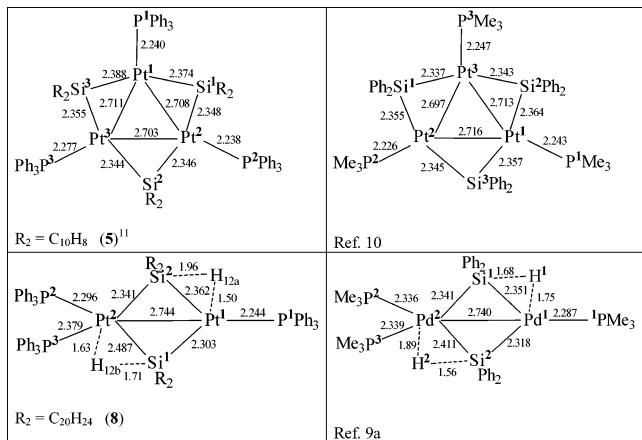


**Figure 7.** Selected bond distances (Å) for **5** and **8** and related complexes. Bond distance data for **8** with esd's are included in Table 2.

The three Pt–Pt bonds in the triangular core of **5** are each bridged by a silafluorenylidene moiety, and one  $\text{PPh}_3$  ligand is bound to each Pt center. The  $\text{Pt}_3\text{Si}_3$  core is nonplanar. The Pt–Si distances in **5** (2.344–2.388 Å) fall in the range for other known Pt–Si complexes (2.34–2.38 Å),<sup>1</sup> and the overall structure is similar to that published for the related complex  $[(\text{Me}_3\text{P})\text{Pt}(\mu\text{-SiPh}_2)]_3$ .<sup>10</sup> The Pt–Pt distances in **5** are in the range for Pt–Pt single bonds in triangular platinum systems (2.70–2.71 Å).<sup>20–22</sup> The Pt–Pt distances in **5** are also similar to those observed in the related cluster  $[(\text{Me}_3\text{P})\text{Pt}(\mu\text{-SiPh}_2)]_3$ .<sup>10</sup>

Trinuclear complexes of Pt containing bridging carbonyl,<sup>21</sup> nitrile, or phosphido<sup>22</sup> ligands are known, but those that incorporate silyl substituents are rare. Recently, Osakada et al. prepared the triplatinum complex  $[(\text{Me}_3\text{P})\text{Pt}(\mu\text{-SiPh}_2)]_3$  from thermolysis of the preformed mononuclear complex  $(\text{Me}_3\text{P})_2\text{Pt}(\text{SiPh}_2\text{H})_2$  at 100 °C.<sup>10</sup> In contrast to the  $\text{Pt}_3\text{Si}_3$  system reported by Osakada, the triplatinum– $\mu$ -silylene complex **5** was generated at room temperature. There are three additional known  $\text{Pt}_3$  systems incorporating a terminal silyl group at a single Pt center. These complexes were synthesized by reaction of a preexisting triplatinum cluster with a hydrosilane, and their structures were confirmed by

(21) For a recent review see: Imhof, D.; Venanzi, L. M. *Chem. Soc. Rev.* **1994**, *23*, 185.

(22) See for example: (a) Bender, R.; Braunstein, P.; Dedieu, A.; Ellis, P. D.; Huggins, B.; Harvey, P. D.; Sappa, E.; Tiripicchio, A. *Inorg. Chem.* **1996**, *35*, 1223. (b) Bennett, M. A.; Berry, D. E.; Dirnberger, T.; Hockless, D. C. R.; Wenger, E. *J. Chem. Soc., Dalton Trans.* **1998**, 2367.

**Table 2.** Selected Bond Distances (Å) and Angles (deg) for **8**

Pt1–Pt2	2.74415(19)	Pt2–Si2	2.3365(9)
Pt1–Si1	2.3035(10)	Pt1–P1	2.2443(9)
Pt1–Si2	2.3626(9)	Pt2–P2	2.2963(9)
Pt2–Si1	2.4875(9)	Pt2–P3	2.3797(9)
Pt1–Si1–Pt2	69.77(3)	P1–Pt1–Si2	144.35(3)
Pt2–Si2–Pt1	71.46(3)	P2–Pt2–Si1	131.13(3)
Si1–Pt1–Si2	111.23(3)	P3–Pt2–Si1	105.76(3)
Si2–Pt2–Si1	105.89(3)	P2–Pt2–Si2	95.21(3)
P2–Pt2–P3	108.50(3)	P3–Pt2–Si2	108.36(3)
P1–Pt1–Pt2	160.92(2)	C1–Si1–C7	90.17(15)
Pt1–Pt2–P3	111.35(2)	C21–Si2–C27	90.42(15)
Pt1–Pt2–P2	135.99(2)		

**Table 3.** Crystal Data and Structure Refinement for **8**

empirical formula	$\text{C}_{101}\text{H}_{103}\text{P}_3\text{Pt}_2\text{Si}_2$
fw	1856.10
temp	150(2) K
wavelength	0.710 73 Å
cryst syst	monoclinic
space group	$P2_1/n$
unit cell dimens	
<i>a</i>	13.6578(2) Å
<i>b</i>	26.7070(3) Å
<i>c</i>	23.6581(3) Å
$\alpha$	90°
$\beta$	91.5540(10)°
$\gamma$	90°
<i>V</i> , <i>Z</i>	8626.33(19) Å <sup>3</sup> , 4
density (calcd)	1.429 Mg/m <sup>3</sup>
abs coeff	3.370 mm <sup>-1</sup>
cryst size	0.22 × 0.16 × 0.10 mm <sup>3</sup>
no. of rflns collected	167 487
no. of indep rflns	24 186 ( <i>R</i> (int) = 0.0574)
completeness to $\theta = 30.00^\circ$	96.1%
abs cor	semiempirical from equivalents (sadabs)
max and min transmission	0.7293 and 0.5243
refinement method	full-matrix least squares on <i>F</i> <sup>2</sup>
no. of data/restraints/params	24 186/1/1032
goodness of fit on <i>F</i> <sup>2</sup>	1.151
final <i>R</i> indices	<i>R</i> 1 = 0.044, <i>wR</i> 2 = 0.065
largest diff peak and hole	1.409 and –1.912 e Å <sup>-3</sup>

X-ray crystallography.<sup>23</sup> Trinuclear complexes of other transition metals with bridging silylene units are also rare.<sup>6</sup>

X-ray-quality crystals of **8** were obtained from slow evaporation of a solution in toluene-*d*<sub>8</sub>. The molecular structure of **8** is shown in Figure 8. Selected bond angles and distances for **8** are listed in Table 2. Table 3 lists the crystal data and structure refinement details for **8**. A molecule of  $\text{C}_7\text{D}_8$  was found in the unit cell lattice and was disordered. The X-ray crystal structure of **8** revealed that the  $\text{Pt}_2\text{Si}_2$  core has one long and three shorter Pt–Si bonds (see Figures 7 and 8). For comparison, the symmetrical dimer  $[(\text{Ph}_3\text{P})\text{Pt}(\mu\text{-}\eta^2\text{-HSiHAr})_2]$  showed alternating long–short Pt–Si bonds, where the long Pt–Si bonds are associated with the  $\text{Pt}\cdots\text{H}\cdots\text{Si}$  interactions.<sup>3b,5e</sup> For example, when Ar = IMP, Pt–Si distances of 2.3248(9) and 2.4280(9) Å were observed and the longer distance corresponded to the Pt–Si bond involved in the nonclassical  $\text{Pt}\cdots\text{H}\cdots\text{Si}$  interaction.<sup>5e</sup>

The Pt–Pt distance in **8** was 2.74415(19) Å, which is slightly longer than the distance found in the sym-

(23) (a) Bender, R.; Braunstein, P.; Bouaoud, S.-E.; Merabet, N.; Rouag, D.; Zanello, P.; Fontani, M. *New. J. Chem.* **1999**, *23*, 1045. (b) Itazaki, N.; Nishihara, Y.; Osakada, K. *Organometallics* **2004**, *23*, 1610.

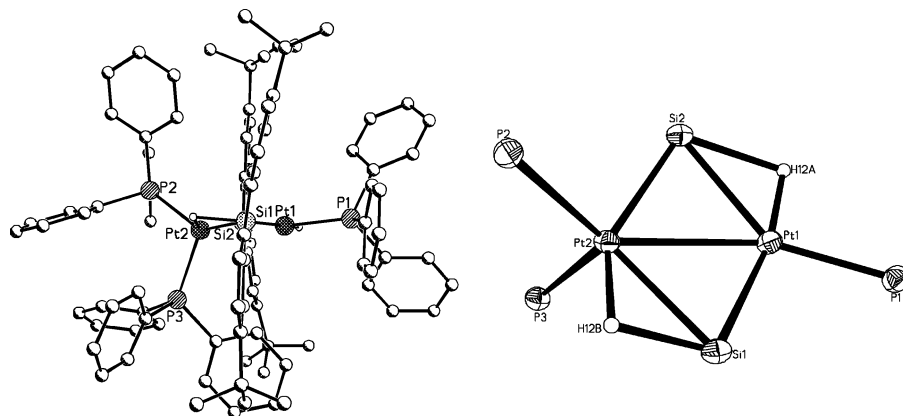


**Figure 8.** (a) Molecular structure of **8**. (b) View of the molecular structure of **8** showing core Pt, P, Si, and H atoms.

metrical dimer  $[(\text{Ph}_3\text{P})\text{Pt}(\mu\text{-}\eta^2\text{-HSiHar})]_2$  (Ar = IMP, 2.7021(2) Å).<sup>5e</sup> This distance is larger than the sum of the covalent platinum radii (2.62 Å)<sup>24</sup> but is within the range for other reported Pt–Pt single bonds.<sup>20,21,22,25</sup>

The hydrides at platinum and silicon were located in **8** from the difference Fourier map and were refined freely. The distances ranged from 1.5 to 1.9 Å. The Pt–H and Si–H distances at the Pt2 center were similar: Pt2–H12b = 1.626 and Si1–H12b = 1.710 Å. These distances suggest a Pt···H···Si bridging environment in the solid state. The Pt2–Si1 distance associated with this hydride is the longest of the four Pt–Si distances. However, in solution this hydride (H12b) appears to adopt a terminal Pt–H site, as indicated by an upfield resonance at –5.2 ppm in the <sup>1</sup>H NMR spectrum (see previous discussion). The remaining hydride, H12a, shows two very different distances to platinum and silicon, Pt1–H12a = 1.503 and Si2–H12a = 1.959 Å, with a Pt1–Si2 distance of 2.36 Å. These distances suggest that this hydride is more closely associated with the Pt1 center than the Si2 center. However, in solution, this hydride appears near 2 ppm, which is in the chemical shift range for reported bridging Pt···H···Si environments.<sup>3b,5g,7</sup>

The related Pd dimer  $(\text{Me}_3\text{P})_2\text{Pd}(\mu\text{-}\eta^2\text{-HSiPh}_2)_2\text{Pd}(\text{PMe}_3)$  showed a similar pattern for the Pd–Si bond lengths, one long and three shorter bonds with similar distances, and the longest distance is analogous to the Pt2–Si1 bond in the current study (see Figure 7).<sup>9a</sup> Both hydrides were described with bridging environments. The palladium–hydride distance associated with the Pd(PMe<sub>3</sub>)<sub>2</sub> unit was the longest distance, Pd2···H2 = 1.89 Å, and the Si–H distance was similar to a typical Si–H bond at Si2···H2 = 1.56 Å,<sup>1</sup> whereas the distances for the Pd(PMe<sub>3</sub>) unit were Pd1···H1 = 1.75 Å and Si1···H1 = 1.68 Å. An interesting difference is observed between the Pt dimer **8** and  $(\text{Me}_3\text{P})_2\text{Pd}(\mu\text{-}\eta^2\text{-HSiPh}_2)_2\text{Pd}(\text{PMe}_3)$ .<sup>9</sup> In the former case, the Pt–H distances are shorter than the Si–H distances but the Pd–H distances are longer than the Si–H distances.

In solution at low temperature, the NMR spectroscopic data for **8** support the presence of a terminal and a bridging hydride. However, the solid-state structure of **8** could contain two bridging hydrides, analogous to

the Pd<sub>2</sub> unsymmetrical dimer reported by Osakada (see above).<sup>9a</sup> One would expect the longest Pt–Si bonds to be associated with nonclassical Pt···H···Si interactions, and on the basis of the Pt···Si bond lengths, it appears that a bridging hydride could be associated with Pt2–Si1 (and Pt1–Si2) for **8** in the solid. However, the shorter Pt1–H12a distance coupled with the elongated Si2–H12a distance indicates that in the solid the hydride could be assigned to a terminal position. Overall, the molecular structure of **8** shows an unusual unsymmetrical environment about the two Pt centers. The hydrides in the Pd dimer<sup>9a</sup> were described by Osakada as bridging hydrides, where H1 was assigned to the triplet and H2 to the doublet signal in the <sup>1</sup>H NMR spectrum, in contrast to our assignments for the hydrides in **8**, where H12b is assigned to the triplet signal.

## Conclusion

Both unsubstituted and substituted silafluorenes (**1** and **6**) reacted with the Pt(0) complex **2** at room temperature to provide initially the mononuclear products  $[(\text{R}_3\text{P})_2\text{Pt}(\text{H})(\text{SiR}_2\text{H})]$  (**3** and **7**), which were identified in solution only and showed similar NMR spectroscopic data. The major species formed in the reaction involving both silafluorenes was an unsymmetrical dimer,  $(\text{Ph}_3\text{P})_2(\text{H})\text{Pt}(\mu\text{-SiR}_2)(\mu\text{-}\eta^2\text{-HSiR}_2)\text{Pt}(\text{PPh}_3)$  (**4** and **8**), both of which were isolated. Attempts to obtain X-ray-quality crystals of complex **4** were unsuccessful; however, the solution NMR data are similar to those of the dimer **8**, whose structure was confirmed by X-ray crystallography. In the case of the unsubstituted silafluorene, a trinuclear complex,  $[(\text{Ph}_3\text{P})\text{Pt}(\mu\text{-SiR}_2)]_3$  (**5**), was formed at room temperature, and its structure was also confirmed by X-ray crystallography. The analogous trimer **9** was observed from a thermal reaction involving the *tert*-butyl-substituted dimer **8**, but to date it has only been observed in solution. The solution <sup>31</sup>P{<sup>1</sup>H} NMR data for **9** are consistent with the data observed for trimer **5**, which supports the assignment of **9** as a trimer. The presence of the *tert*-butyl groups on the silafluorene unit appear to impart added solubility to the trimer **9** relative to the unsubstituted system **5**. Attempts to grow X-ray-quality crystals of **9** are in progress.

Further studies with other constrained secondary hydrosilanes are planned, to determine if such silicon

(24) Pauling, L. *The Nature of the Chemical Bond*, 3rd ed.; Cornell University Press: Ithaca, NY, 1960; p 224.

(25) Green, M.; Howard, J. A. K.; Proud, J.; Spencer, J. L.; Stone, F. G. A.; Tsipis, C. A. *J. Chem. Soc., Chem. Commun.* **1976**, 671.

systems will generate trinuclear or higher order polynuclear clusters (as well as their mechanism of formation). It is expected that other silicon ring systems will exhibit monomer/dimer/trimer species, and we expect to probe the sequence of molecular events that occur from monomer to dimer and/or trimer. It is probable that there is more than one pathway by which the trimer or higher aggregates are formed.

### Experimental Section

All glassware was oven- or flame-dried prior to use. Reactions were performed under an argon or nitrogen atmosphere. Melting point determinations were obtained on a Thomas-Hoover capillary melting point apparatus and are uncorrected. Infrared spectra were recorded on a Thermo-Nicolet Avatar 360 ESP FT-IR spectrometer.  $^1\text{H}$ ,  $^{29}\text{Si}$ , and  $^{31}\text{P}$  NMR spectra were recorded on a Bruker ARX-500 spectrometer at 500 MHz for  $^1\text{H}$ , 99 MHz for  $^{29}\text{Si}$ , and 202 MHz for  $^{31}\text{P}$ . Proton chemical shifts ( $\delta$ ) are reported relative to residual protonated solvent,  $\text{C}_7\text{D}_8$  (2.09 ppm), and  $\text{CD}_2\text{Cl}_2$  (5.32 ppm). Silicon chemical shifts ( $\delta$ ) are reported relative to external TMS (0 ppm). Phosphorus chemical shifts ( $\delta$ ) are reported relative to external  $\text{H}_3\text{PO}_4$  (0 ppm). Chemical shifts are given in ppm and coupling constants in Hz. Both  $^{29}\text{Si}\{^1\text{H}\}$  and  $^{31}\text{P}\{^1\text{H}\}$  NMR spectroscopic data for compounds **3–5** and **7–9** are listed in Table 1. The Pt–H and/or Si–H resonances in the  $^1\text{H}$  NMR spectra for compounds **3**, **4**, **7**, and **8** are also given in Table 1. X-ray crystal structural determinations were performed on a Bruker SMART diffractometer equipped with a CCD area detector.

Silafluorene<sup>12</sup> and 3,7-di-*tert*-butylsilafluorene<sup>13</sup> were prepared as described previously. (Ethylene)bis(triphenylphosphine)platinum(0) was purchased from Aldrich Chemical Co. and used as received. Toluene-*d*<sub>8</sub> was purchased in 1 g ampules from Cambridge Isotopes, Inc., and used as received.

**Reaction of Silafluorene (1) with  $(\text{Ph}_3\text{P})_2\text{Pt}(\eta^2\text{-C}_2\text{H}_4)$  (2). Isolation of  $[(\text{Ph}_3\text{P})\text{Pt}(\mu\text{-SiC}_{12}\text{H}_8)]_3$  (5).** Silafluorene (**1**; 73 mg, 0.34 mmol) was added to  $(\text{Ph}_3\text{P})_2\text{Pt}(\eta^2\text{-C}_2\text{H}_4)$  (**2**; 250 mg, 0.34 mmol) in a 20 mL vial, and then  $\text{C}_6\text{D}_6$  (1.5 mL) and  $\text{C}_6\text{H}_6$  (3.5 mL) were added, resulting in a clear, amber red solution. After several hours, red crystals of **5** had precipitated, which were separated. Addition of hexane (8 mL) to the mother liquor resulted in precipitation of an additional crop of **5**. The solid sample of **5** (as the bis solvate) was dried under vacuum for 2 h to give a total of 64 mg (27% yield based on Pt).  $^1\text{H}$  NMR (500 MHz,  $\text{CD}_2\text{Cl}_2$ , room temperature):  $\delta$  7.40 (d,  $^3J_{\text{HH}} = 7.6$ ), 7.06 (t,  $^3J_{\text{HH}} = 7.3$ ), 6.95–6.87 (m), 6.07 (t,  $^3J_{\text{HH}} = 7.6$ ) ArH. Anal. Calcd for  $\text{C}_{90}\text{H}_{69}\text{P}_3\text{Pt}_3\text{Si}_3\cdot 2\text{C}_6\text{H}_6$ : C, 59.21; H, 3.95. Found: C, 59.32; H, 4.11. The remaining solution was evaporated to give a chocolate brown solid (199 mg) as a mixture of components. Low-temperature  $^{31}\text{P}\{^1\text{H}\}$  NMR in toluene-*d*<sub>8</sub> indicated that the mixture contained mainly  $(\text{Ph}_3\text{P})_3\text{Pt}$ ,  $(\text{Ph}_3\text{P})_4\text{Pt}$ , and  $\text{Ph}_3\text{PO}$  with chemical shifts at  $\delta$  52.3 (s, Pt satellites,  $J_{\text{PtP}} = 4440$ ), 11.7 (s, Pt satellites,  $J_{\text{PtP}} = 3840$ ), and 27.1 (s).<sup>26</sup>

**Isolation of  $(\text{Ph}_3\text{P})_2(\text{H})\text{Pt}(\mu\text{-SiC}_{12}\text{H}_8)(\mu\text{-}\eta^2\text{-HSiC}_{12}\text{H}_8)\text{Pt}(\text{PPh}_3)$  (4).** In a drybox, silafluorene (**1**; 11 mg, 0.060 mmol) was dissolved in  $\sim 0.25$  mL of  $\text{C}_7\text{D}_8$ . In an NMR tube,  $(\text{PPh}_3)_2\text{Pt}(\eta^2\text{-C}_2\text{H}_4)$  (**2**; 41 mg, 0.055 mmol) was dissolved in  $\sim 0.75$  mL of  $\text{C}_7\text{D}_8$  and placed in liquid  $\text{N}_2$ . The silafluorene solution was then added to the frozen  $(\text{Ph}_3\text{P})_2\text{Pt}(\eta^2\text{-C}_2\text{H}_4)$  solution. After the additional sample had frozen, the tube was removed to a dry ice/acetone bath, and when the matrix melted, the reaction tube was shaken several times to mix the contents and then placed into a precooled NMR magnet (193 K). The temperature was slowly raised to 300 K over a period of several hours. After approximately 7 h,  $^{31}\text{P}\{^1\text{H}\}$  NMR and  $^1\text{H}$  NMR data showed the presence of dimer **4** as the major species. The solution was

then transferred to a vial in the drybox, where  $\sim 5$  mL of pentane was added, and the sample was stored several days at  $-40$  °C, whereupon a dark orange solid formed. The solution was filtered and the solid dried in vacuo to give **4** (19 mg, 45% yield based on Pt, mp 214 °C dec). NMR spectroscopic data for **4**:  $^1\text{H}$  NMR ( $\text{C}_7\text{D}_8$ , 500 MHz, 223 K)  $\delta$  8.0–6.6 (overlapping aromatic resonances);  $^{31}\text{P}\text{-}^{31}\text{P}\{^1\text{H}\}$  COSY (223 K, 500 MHz) cross-peak correlation observed between peak at 31.1 ppm with peak at 17.3 ppm;  $^1\text{H}\text{-}^{31}\text{P}$  COSY (223 K, 500 MHz) correlation between hydride peak at  $-4.9$  ppm with phosphorus resonance at 17.3, correlation between hydride peak at 2.0 with phosphorus resonance at 31.1 ppm. Anal. Calcd for  $\text{C}_{78}\text{H}_{63}\text{P}_3\text{Pt}_2\text{-Si}_2$ : C, 60.85; H, 4.12. Found: C, 61.18; H, 4.34.

**Observation of  $(\text{Ph}_3\text{P})_2\text{Pt}(\text{H})[\text{Si}(\text{C}_{12}\text{H}_8)\text{H}]$  (3).** In a typical run, **1** and **2** were mixed in  $\text{C}_7\text{D}_8$  (1:1 ratio). NMR spectroscopic data were collected at room temperature immediately after addition. Complex **3** was characterized in solution only, since its lifetime was approximately 30 min. Attempts to confirm the Si–H assignment (room temperature) at 5.1 ppm by 2D NMR experiments failed, due to the limited lifetime of **3**. A sample containing **3** was cooled to  $-50$  °C, and  $^1\text{H}$  NMR data were obtained.

**Reaction of 3,7-Di-*tert*-butylsilafluorene (6) with  $(\text{Ph}_3\text{P})_2\text{Pt}(\eta^2\text{-C}_2\text{H}_4)$  (2).** In a drybox, 3,7-di-*tert*-butylsilafluorene (**6**; 20.0 mg, 0.068 mmol) in  $\text{C}_7\text{D}_8$  (0.5 mL) was added to  $(\text{Ph}_3\text{P})_2\text{Pt}(\eta^2\text{-C}_2\text{H}_4)$  (**2**; 50.0 mg, 0.067 mmol) in  $\text{C}_7\text{D}_8$  (0.5 mL), resulting in gas evolution and formation of a dark amber solution. Slow evaporation of the solvent (over several days) resulted in precipitation of bright orange crystals of **8** as a toluene solvate (54 mg, yield 86% based on Pt), mp 186–192 °C dec. Crystals of **8** were washed with toluene-*d*<sub>8</sub> and were suitable for X-ray crystallographic analysis.  $^1\text{H}$  NMR ( $\text{C}_7\text{D}_8$ , 500 MHz, 223 K):  $\delta$  8.4–6.3 (overlapping multiplets, ArH region), 1.34 (s,  $\text{C}(\text{CH}_3)_3$ ), 1.03 (broad s,  $\text{C}(\text{CH}_3)_3$ ).  $^{31}\text{P}\text{-}^{31}\text{P}\{^1\text{H}\}$  COSY (223 K, 500 MHz): cross-peak correlation observed between peak at 30.3 ppm with peak at 21.5 ppm.  $^1\text{H}\text{-}^{31}\text{P}$  COSY (223 K, 500 MHz): correlation between hydride peak at  $-5.2$  ppm with phosphorus resonance at 21.5 ppm; correlation between hydride peak at 1.93 ppm with phosphorus resonance at 30.3 ppm. Anal. Calcd for  $\text{C}_{94}\text{H}_{95}\text{P}_3\text{Si}_2\text{Pt}_2\text{-C}_7\text{D}_8$ : C, 65.36; H, 5.59. Found: C, 65.40; H, 5.60.

A sample of **8** was heated in  $\text{C}_7\text{D}_8$  in the probe of the NMR spectrometer in 20 K increments from ambient temperature to 360 K and held at that temperature for approximately 1 h with no observable decomposition, as determined by cooling the sample to 223 K and monitoring by  $^1\text{H}$  and  $^{31}\text{P}$  NMR for resonances associated with **8**. Additional heating at 373 K overnight provided a new resonance with platinum satellites, in the  $^{31}\text{P}$  spectrum. This new resonance has tentatively been assigned to the trinuclear system **9**, analogous to **5**.<sup>11</sup> Loss of the broad room-temperature resonance for **8** also occurred.

**X-ray Crystallographic Analysis of 8.** A crystal (obtained from slow evaporation of  $\text{C}_7\text{D}_8$ ) with approximate dimensions  $0.22 \times 0.16 \times 0.10$  mm was mounted on glass fibers in a random orientation. Preliminary examination and data collection were performed using a Bruker SMART charge coupled device (CCD) detector system single-crystal X-ray diffractometer. SMART and SAINT software packages (Bruker Analytical X-ray, Madison, WI, 2002) were used for data collection ( $\omega$  and  $2\theta$  scans) and data integration. Collected data were corrected for systematic errors using SADABS.<sup>27</sup>

Collection parameters for crystal data collection are listed in Table 3 and in the Supporting Information. Structure solution and refinement were carried out using the SHELXTL-PLUS software package.<sup>28</sup> The structure was solved by Patterson methods and refined successfully in the space group  $P2_1/n$ . The non-hydrogen atoms were refined anisotropically to

(27) Blessing, R. H. *Acta Crystallogr.* **1995**, *A51*, 33.

(28) Sheldrick, G. M. Bruker Analytical X-ray Division, Madison, WI, 2002.



convergence. The two bridging H atoms were located from the difference Fourier and were refined freely. The rest of the hydrogen atoms were treated using an appropriate riding model (AFIX m3). A molecule of toluene was found in the crystal lattice. The toluene solvate exhibits rotational disorder. The disorder was resolved by locating two partial molecules, which were refined as rigid bodies.

**Acknowledgment.** We are grateful for a grant from the National Science Foundation (Grant No. CHE-0316023) for support of this work. The support of the

NSF (Grant No. CHE-9974801) and an UM-Research Board grant for the purchase of a Bruker Avance 300 NMR spectrometer are gratefully acknowledged.

**Supporting Information Available:** Selected NMR spectroscopic data and crystallographic data for **8**, including tables of crystal data and structure refinement details, atomic coordinates, and bond distances and angles. This material is available free of charge via the Internet at <http://pubs.acs.org>.

OM0400447